

## PDF hosted at the Radboud Repository of the Radboud University Nijmegen

The following full text is a publisher's version.

For additional information about this publication click this link.

<http://repository.ubn.ru.nl/handle/2066/127871>

Please be advised that this information was generated on 2018-02-15 and may be subject to change.



## Laser induced spin precession in highly anisotropic granular L10 FePt

J. Becker, O. Mosendz, D. Weller, A. Kirilyuk, J. C. Maan, P. C. M. Christianen, Th. Rasing, and A. Kimel

Citation: [Applied Physics Letters](#) **104**, 152412 (2014); doi: 10.1063/1.4871869

View online: <http://dx.doi.org/10.1063/1.4871869>

View Table of Contents: <http://scitation.aip.org/content/aip/journal/apl/104/15?ver=pdfcov>

Published by the [AIP Publishing](#)

---

### Articles you may be interested in

[Spin-orbit interaction tuning of perpendicular magnetic anisotropy in L10 FePdPt films](#)

Appl. Phys. Lett. **104**, 192402 (2014); 10.1063/1.4876128

[Low energy C+ ion embedment induced structural disorder in L10 FePt](#)

J. Appl. Phys. **115**, 013907 (2014); 10.1063/1.4860295

[Ultrafast laser-induced magnetization precession dynamics in FePt/CoFe exchange-coupled films](#)

Appl. Phys. Lett. **97**, 172508 (2010); 10.1063/1.3510473

[Photoinduced magnetic softening of perpendicularly magnetized L10-FePt granular films](#)

Appl. Phys. Lett. **93**, 162509 (2008); 10.1063/1.3007977

[Phase separation and nanoparticle formation in Cr-dosed FePt thin films](#)

J. Appl. Phys. **101**, 053901 (2007); 10.1063/1.2436926

---

Agilent's Electronic Measurement Group is becoming **Keysight Technologies**.



**Engineering Education & Research Resources DVD 2014**

Agilent is the key to your test and measurement needs **Order yours**



## Laser induced spin precession in highly anisotropic granular L1<sub>0</sub> FePt

J. Becker,<sup>1,2</sup> O. Mosendz,<sup>3</sup> D. Weller,<sup>3</sup> A. Kirilyuk,<sup>1</sup> J. C. Maan,<sup>2</sup> P. C. M. Christianen,<sup>2</sup> Th. Rasing,<sup>1</sup> and A. Kimel<sup>1</sup>

<sup>1</sup>Radboud University Nijmegen, Institute for Molecules and Materials, Nijmegen 6525 AJ, The Netherlands

<sup>2</sup>High Field Magnet Laboratory, Institute for Molecules and Materials, Radboud University Nijmegen, Toernooiveld 7, 6525 ED Nijmegen, The Netherlands

<sup>3</sup>HGST, a Western Digital company, 3403 Yerba Buena Road, San Jose, California 95135, USA

(Received 1 February 2014; accepted 8 April 2014; published online 17 April 2014)

The dynamic magnetic properties of a highly anisotropic, granular L1<sub>0</sub> FePt thin film in magnetic fields up to 7 T are investigated using time-resolved magneto-optical Kerr effect measurements. We find that ultrashort laser pulses induce coherent spin precession in the granular FePt sample. Frequencies of spin precession up to over 400 GHz are observed, which are strongly field and temperature dependent. The high frequencies can be ascribed to the high value of the magnetocrystalline anisotropy constant  $K_u$  leading to large anisotropy fields  $H_a$  of up to 10.7 T at 170 K. A Gilbert damping parameter of  $\alpha \sim 0.1$  was derived from the lifetimes of the oscillations.

© 2014 Author(s). All article content, except where otherwise noted, is licensed under a Creative Commons Attribution 3.0 Unported License. [<http://dx.doi.org/10.1063/1.4871869>]

The dynamics of spins in magnetic materials triggered by a subpicosecond laser pulse is a recently emerging and rapidly developing area in fundamental magnetism.<sup>1–4</sup> The ultimate practical goal of this research is to learn how to control the magnetic state of a medium on an ultrafast timescale. Several mechanisms of such a laser-induced switching have been suggested. For ferrimagnetic metallic alloys, such as GdFeCo, it was shown that a subpicosecond laser excitation can trigger magnetization reversal via a strongly non-equilibrium state with no net magnetization.<sup>5–7</sup> For ferromagnetic materials, another mechanism of reversible switching of the magnetization was suggested.<sup>8,9</sup> In this mechanism, the switching proceeds via coherent spin precession triggered by a subpicosecond laser pulse.

Despite the claimed importance of the research for magnetic recording technologies, most studies treating laser-induced magnetization dynamics have been focused on continuous metallic films with relatively low values of magnetic anisotropy ( $K_u < 10^7$  erg/cm<sup>3</sup>). On the other hand, state-of-the-art recording media are based on granular ferromagnetic compounds featuring high anisotropy values ( $K_u > 10^7$  erg/cm<sup>3</sup>), such as FePt,<sup>10</sup> in order to increase the data storage density. The high magnetocrystalline anisotropy in these materials could lead to spin precession in the THz regime. However, since the nm-sized grains are exchange decoupled and have a certain spread in size and crystallographic orientation, it is not known whether a  $\mu$ m-sized laser excitation will result in a collective, coherent response of their spins. Hence, a possible ultrafast control of the magnetization depends crucially on whether subpicosecond laser excitations can trigger coherent spin dynamics in such a granular compound. In this paper, we demonstrate that this is indeed the case, using a time-resolved magneto-optical Kerr effect (TR-MOKE) technique on a sample of highly anisotropic, granular FePt. We furthermore show that the observed frequencies indeed reach hundreds of GHz.

The investigated sample is a granular FePt thin film. It was grown by sputter deposition at a substrate temperature of 550 °C on a set of underlayers with MgO (001) surfaces

directly beneath the FePt, resulting in an out of plane easy axis of magnetization (for more information see Ref. 11). The elevated growth temperature leads to the formation of the face centered tetragonal (fct) L1<sub>0</sub> phase rather than the face centered cubic (fcc) A1 phase.<sup>12,13</sup> The L1<sub>0</sub> phase is chemically ordered (chemical order parameter  $S = 1$ ), as atomic layers of Fe and Pt alternate along the [001] direction. It has been shown that in contrast to the fcc phase, the fct phase has a high magnetocrystalline anisotropy of  $K_u \sim 7 \times 10^7$  erg/cm<sup>3</sup>.<sup>14</sup> Thus, the higher the chemical ordering in the FePt layer, the higher the magnetocrystalline anisotropy.<sup>15</sup> The cubic MgO-(001) seed layer provides a correct template for FePt crystal growth, while a slightly larger lattice parameter of MgO stretches the FePt a-axis. The FePt/MgO interface induced stress in combination with the tetragonal nature of the FePt L1<sub>0</sub> crystal results in a desired configuration with in-plane orientation of the hard magnetic a-axis and the easy magnetic c-axis in the out of plane direction. Even though X-ray diffraction measurements have confirmed a high degree of chemical ordering in this sample, structural defects such as mis-oriented grains cause a slight reduction of the overall order in the sample.<sup>11</sup> To ensure magnetically decoupled, separate grains, 35 vol. % of carbon is added as a segregant during the growth process. Carbon does not coalesce with FePt hence forming physically isolated and exchange decoupled grains of roughly 7 nm diameter and a grain size distribution of  $\sigma = 16\%$ .<sup>11</sup> The magnetic layer is capped by a 3 nm thick protective diamond like carbon (DLC) overcoat,<sup>16</sup> allowing for optical access.

To characterize the static magnetic properties of the sample, the polar magneto-optical Kerr effect was measured at a wavelength of 800 nm. Magnetic hysteresis loops were recorded applying an external magnetic field along the easy axis of magnetization, normal to the sample plane. The resulting hysteresis loops (Fig. 1) reveal a high coercive field ( $H_c$ ) of  $5.0 \pm 0.1$  T at room temperature. Decreasing the temperature to 4.2 K leads to a significant increase in coercive field to  $8.2 \pm 0.5$  T. To saturate the magnetization at 4.2 K, fields greater than  $H_s = 11 \pm 0.5$  T are required. This increase



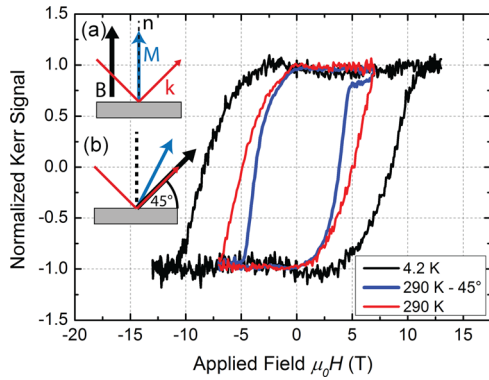


FIG. 1. Hysteresis loops acquired using the polar MOKE at 290 K (red curve) and 4.2 K (black curve). Inset (a) shows the polar measurement geometry (red and black curve) while (b) shows the 45° geometry (blue curve). The high coercive field  $H_c = 5$  T at 290 K is increased to 8.2 T at 4.2 K. Applying the field at a 45° angle to the easy axis results in a reduced  $H_c = 3.7$  T.

in  $H_c$  and  $H_s$  can be attributed to an increase in anisotropy at lower temperatures<sup>15</sup> as is also confirmed by our measurements of the magnetization dynamics (see below). The rather wide switching field distribution that can be observed in the hysteresis curves can be explained with structural (grain size distribution) and chemical ( $S < 1$ ) inhomogeneities.<sup>11</sup> Another notable effect was observed when applying the external field at a 45° angle with respect to the sample normal. In this configuration, the coercive field is reduced to  $3.7 \pm 0.1$  T. This effect can be attributed to the granular nature of the FePt layer. The individual grains are single domain, exchange decoupled ferromagnets which can be described by a Stoner-Wohlfarth (SW) model.<sup>17</sup> For ideal SW particles, the switching field is minimal if applied between the hard and easy axis of magnetization which corresponds to a 45° angle for the here presented sample.

In order to investigate the dynamic magnetic properties, we used an all optical, TR-MOKE pump probe technique described elsewhere.<sup>4</sup> The sample was excited with a 100 fs light pulse at a central wavelength of 800 nm and a fixed fluence of  $0.4 \text{ mJ/cm}^2$ . It was subsequently probed with a similar pulse 100 times lower in power. During the measurement, an external magnetic field up to 7 T was applied at an angle of 45° with the sample normal. A measurement at room temperature and an applied magnetic field of 7 T is shown in Fig. 2(a). The laser pulse excitation leads to an initial ultrafast demagnetization within 1.5 ps. The point of maximum demagnetization is defined as zero on the x-axis. Following the demagnetization, a relaxation of the magnetization is observed, overlaid by an oscillation. The overall re-magnetization can be described by a bi-exponential function  $f(t) = f(0) - A_1 \exp(-t/\tau_1) - A_2 \exp(-t/\tau_2)$  with amplitudes  $A_1, A_2$ . The lifetimes  $\tau_1$  and  $\tau_2$  represent the typical timescales of the relaxation of the spin temperature and heat diffusion away from the irradiated site, respectively. Our measurements yielded a typical value for  $\tau_1 \sim 1.5$  ps, whereas  $\tau_2 > 25$  ps cannot be accurately determined as the data only extend to delay values of 16 ps. This background re-magnetization at positive  $\Delta t$  was subtracted in Fig. 2(b) to present the oscillatory part only. A damped sine function  $A_0 \exp(-t/\tau_L) \sin(2\pi f t - \phi)$  is used as a fitting function, with  $A_0, \tau_L, f$ , and  $\phi$  representing amplitude, lifetime, frequency,

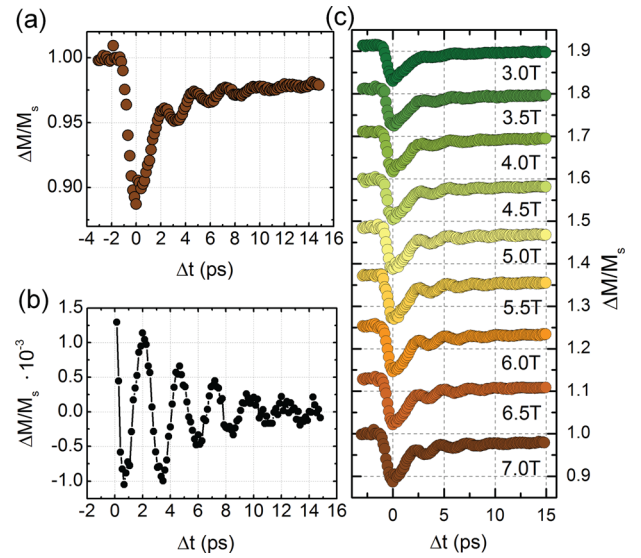


FIG. 2. (a) TR-MOKE time trace on FePt at 290 K, 7 T. Following the initial demagnetization, damped oscillations are visible during the magnetization relaxation, even more so if the exponential contribution of the relaxation is subtracted (b). (c) TR-MOKE data at 290 K at different applied magnetic fields ranging from 7 T down to 3 T.

and phase of the oscillation, respectively. Only data for positive  $\Delta t$  are considered for the fitting. This yields a frequency of  $\sim 385$  GHz for the room temperature measurement at 7 T applied field. To investigate whether ferromagnetic resonance (FMR) is observed here, measurements at different applied magnetic fields at temperatures of 290 K (Fig. 2(c)) and 170 K (not shown) were performed. Starting with a magnetically saturated sample at 7 T, the magnetization dynamics were measured reducing the field in steps of 0.25 T down to 3 T. The oscillations show a monotonic decrease in frequency as the applied magnetic field is reduced (squares in Fig. 3), which is to be expected for FMR. At 170 K (circles in Fig. 3), similar behaviour is observed, but shifted to even higher frequencies of up to  $\sim 430$  GHz at 7 T. Both data sets are fitted (orange and blue lines in Fig. 3) according to the frequency-field relationship for ferromagnetic resonance, derived from the Landau-Lifshitz(-Gilbert) (LLG) formula

$$\frac{d\mathbf{M}}{dt} = \gamma \mathbf{M} \times \mathbf{H}_{\text{eff}} + \frac{\alpha}{M} \left( \mathbf{M} \times \frac{d\mathbf{M}}{dt} \right), \quad (1)$$

with the gyromagnetic ratio  $\gamma = g\mu_B/\hbar$ , g-factor  $g$ , Bohr magneton  $\mu_B$ , effective field  $\mathbf{H}_{\text{eff}} = -\delta U/\delta \mathbf{M}$ , the damping parameter  $\alpha$ , the saturation magnetization  $M$ , and the internal magnetic energy  $U$ . For a thin film with out of plane anisotropy, taking into account the Zeeman energy, demagnetization energy, the uniaxial anisotropy energy, and the internal magnetic energy can be written as follows:

$$U = -\mathbf{M} \cdot \mathbf{H} + 2\pi(\mathbf{M} \cdot \mathbf{n})^2 - \frac{K_u}{M^2}(\mathbf{M} \cdot \mathbf{u})^2, \quad (2)$$

with applied magnetic field  $\mathbf{H}$ , the sample normal  $\mathbf{n}$ , and the easy axis vector  $\mathbf{u}$ . Here, the sample is considered as a continuous film, neglecting a possible reduction of the demagnetizing fields due to the granular structure. However, the effect of this reduction on  $U$  is small as the spherical grains

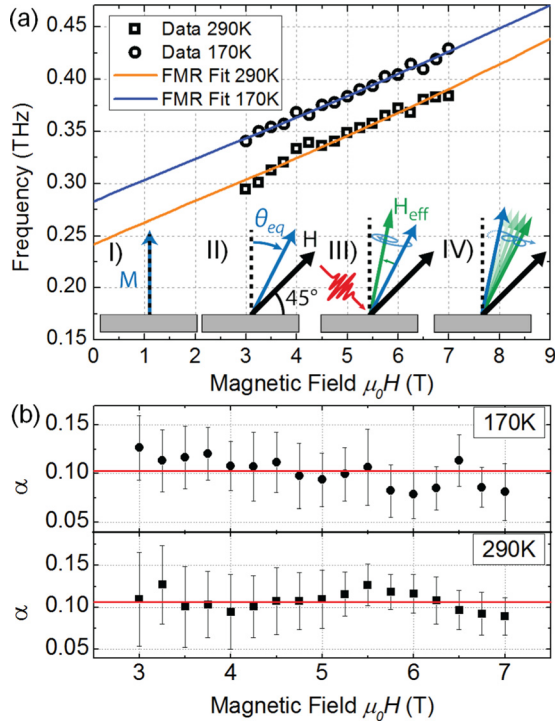


FIG. 3. (a) Magnetic field dependence of the extracted frequency at 290 K (black squares) and 170 K (black circles). The respective FMR fits are given by the orange (290 K) and blue (170 K) curves. Insets I) to IV): schematic illustration of the magnetization and effective field behaviour without applied field (I), with applied field (II), at pump excitation (III), and following dynamic response (IV). (b) Extracted values for the damping parameter  $\alpha$  (red lines indicate mean value) for 290 K and 170 K.

occupy 65 vol. % of the film and due to the high  $K_u$ , the anisotropy energy will be significantly higher than the demagnetizing energy. Using spherical coordinates, the equilibrium angles for the magnetization  $\mathbf{M}$ ,  $\theta_{eq}$ , and  $\varphi_{eq}$ , that minimize  $U$  are then given by

$$\frac{\sin(\theta_{eq} - \theta_h)}{\sin 2\theta_{eq}} = \frac{4\pi M - 2K_u/M}{2H}, \quad \cos \varphi_{eq} = 0, \quad (3)$$

with  $\theta_h$  is the polar angle of the applied magnetic field  $\mathbf{H}$  relative to the sample normal. For the magnetization  $\mathbf{M}$ , time dependent azimuthal and polar angles  $\theta$ ,  $\varphi \sim e^{i\omega t}$ , and small oscillation amplitudes around the equilibrium are assumed. This yields the following formula for ferromagnetic resonance from Eq. (1):

$$\frac{\omega^2}{\gamma^2} = H_1 \cdot H_2, \quad (4)$$

$$\begin{aligned} H_1 &= H \cos(\theta_{eq} - \theta_h) - (4\pi M - 2K_u/M) \cos^2 \theta_{eq} \\ H_2 &= H \cos(\theta_{eq} - \theta_h) - (4\pi M - 2K_u/M) \cos 2\theta_{eq}. \end{aligned} \quad (5)$$

Using the measured saturation magnetization for this sample of  $950 \text{ emu/cm}^3$  at room temperature, the fit yields values for the anisotropy fields and the g-factor as shown in Table I. The anisotropy field found at room temperature is not equal to the coercive field, as theory would predict for ideal Stoner-Wohlfarth particles. Here, however, a great ensemble of grains is measured. The grains in the FePt sample have slightly differing shapes and are spread in size as well

TABLE I. Results of the FMR-fit for 290 K and 170 K.

Temperature (K)	g-factor	$H_{an}$ (T)
290	$2.2 \pm 0.1$	$8.9 \pm 0.3$
170	$2.2 \pm 0.1$	$10.7 \pm 0.3$

as in crystalline alignment, thus showing merely near-SW behaviour.<sup>18</sup> We find that the anisotropy field  $H_{an} = 2K_u/M$  increases with decreasing temperature. It is known for L1<sub>0</sub> FePt that with decreasing temperature,  $K_u$  increases stronger than  $M$ .<sup>15</sup>

If one extrapolates the fit towards zero applied field (Fig. 3(a)), the FMR frequency does not drop to zero but reaches a value of  $\sim 240 \text{ GHz}$  at room temperature ( $\sim 280 \text{ GHz}$  at 170 K). As can be seen from Eqs. (4) to (5), the magnitude of this zero field frequency is determined by the demagnetizing field  $4\pi M$  and the anisotropy field  $2K_u/M$  acting against each other. At room temperature, the demagnetizing field equals  $\sim 1.2 \text{ T}$ , which is small compared to the anisotropy field of  $8.9 \text{ T}$ . This leads to the conclusion that the strong magnetocrystalline anisotropy  $K_u$  is responsible for the high frequencies of spin precession. As  $K_u$  has a stronger temperature dependence than  $M$ ,<sup>15</sup> the shift in the frequency observed between the measurements at 290 K and 170 K can likewise be ascribed to the increase of  $K_u$  with decreasing temperature.

The light induced excitation of coherent spin precession can be explained phenomenologically. Initially, the magnetization points along the out of plane easy axis (Fig. 3(a-I)). After applying an external field  $\mathbf{H}$ , the magnetization aligns along the effective field at an angle  $\theta_{eq}$  (see Eq. (3)) between the easy axis and the direction of the applied field (Fig. 3(a-II)). Upon pump arrival, two possible processes can initiate the above seen coherent spin precession: An ultrafast demagnetization, decreasing the Zeeman and demagnetization energy, or an ultrafast change of the magnetocrystalline anisotropy  $K_u$ . In both cases, the effective field  $\mathbf{H}_{eff}$  is tilted out of its equilibrium position (Fig. 3(a-III)), so it does not lie parallel to  $\mathbf{M}$  anymore. This creates a torque that acts on the magnetization, thereby starting the precessional motion around  $\mathbf{H}_{eff}$  which also relaxes back to its initial position as the energy is dissipated (Fig. 3(a-IV)).

Furthermore, by evaluating the lifetimes  $\tau_L$  of the oscillations the damping parameter  $\alpha$  can be extracted, using the following relationship derived from the LLG equation assuming that  $\alpha \ll 1$ :

$$\alpha = \frac{2}{\tau_L \gamma (H_1 + H_2)}. \quad (6)$$

A damping factor of  $\alpha \sim 0.1$  is obtained for measurements at 290 K as is shown in Fig. 3(b). No significant change in  $\alpha$  above the experimental error is observed upon reducing the temperature to 170 K. Also, the damping does not change notably as a function of applied magnetic field. This suggests that there is only little (if any) extrinsic contribution to the measured Gilbert damping parameter. Indeed, strong external magnetic fields as applied here are known to suppress extrinsic damping.<sup>19,20</sup> Similar relatively high values for the

intrinsic Gilbert damping parameter were reported on continuous FePt films with lower magnetocrystalline anisotropy.<sup>21–23</sup>

In summary, our here presented results show that coherent spin precession can be excited in a highly anisotropic, granular L1<sub>0</sub> FePt films using ultrashort light pulses of 100 fs. The high anisotropy fields up to more than 10 T found in the here investigated sample lead to FMR frequencies in the THz range. Frequencies of that magnitude have never before been observed in ferromagnets, and are of considerable relevance to the writing speed in magnetic data storage: Considering conventional damped gyroscopic switching, where the switching field is applied parallel to the easy axis, the switching time is inversely proportional to the frequency of magnetization precession. Lowering the temperature increases the magnetocrystalline anisotropy  $K_u$  which leads to a substantial increase in the observed precession frequency. Furthermore, a Gilbert damping parameter of  $\alpha \sim 0.1$  is found, similar to results for continuous films of L1<sub>0</sub>.

The authors would like to thank A. Toonen, A. van Etteger, and P. Albers for technical support and R. Subkhangulov for his assistance with the measurements. This research was partially supported by de Nederlandse Organisatie voor Wetenschappelijk Onderzoek (NWO), de Stichting voor Fundamenteel Onderzoek der Materie (FOM), the European Union's Seventh Framework Program (FP7/2007-2013) Grant No. 281043 (FemtoSpin), and the European Union's Seventh Framework Program (FP7/2007-2013)/ERC Grant Agreement No. 257280 (Femtomagnetism). Part of this work was also supported by EuroMagNET II under the EU Contract No. 228043. We acknowledge the support of the HFML-RU/FOM, member of the European Magnetic Field Laboratory (EMFL)).

<sup>1</sup>E. Beaupaire, J.-C. Merle, A. Daunois, and J.-Y. Bigot, *Phys. Rev. Lett.* **76**, 4250 (1996).

<sup>2</sup>J. Hohlfeld, E. Matthias, R. Knorren, and K. H. Bennemann, *Phys. Rev. Lett.* **78**, 4861 (1997).

- <sup>3</sup>B. Koopmans, M. van Kampen, J. T. Kohlhepp, and W. J. M. de Jonge, *Phys. Rev. Lett.* **85**, 844 (2000).
- <sup>4</sup>A. Kirilyuk, A. V. Kimel, and T. Rasing, *Rev. Mod. Phys.* **82**, 2731 (2010).
- <sup>5</sup>K. Vahaplar, A. M. Kalashnikova, A. V. Kimel, D. Hinzke, U. Nowak, R. Chantrell, A. Tsukamoto, A. Itoh, A. Kirilyuk, and T. Rasing, *Phys. Rev. Lett.* **103**, 117201 (2009).
- <sup>6</sup>I. Radu, K. Vahaplar, C. Stamm, T. Kachel, N. Pontius, H. A. Dürr, T. A. Ostler, J. Barker, R. F. L. Evans, R. W. Chantrell, A. Tsukamoto, A. Itoh, A. Kirilyuk, T. Rasing, and A. V. Kimel, *Nature* **472**, 205 (2011).
- <sup>7</sup>T. Ostler, J. Barker, R. Evans, R. Chantrell, U. Atxitia, O. Chubykalo-Fesenko, S. El Moussaoui, L. Le Guyader, E. Mengotti, L. Heyderman, F. Nolting, A. Tsukamoto, A. Itoh, D. Afanasiev, B. Ivanov, A. Kalashnikova, K. Vahaplar, J. Mentink, A. Kirilyuk, T. Rasing, and A. Kimel, *Nat. Commun.* **3**, 666 (2012).
- <sup>8</sup>E. Carpena, E. Mancini, C. Dallera, E. Puppini, and S. De Silvestri, *J. Appl. Phys.* **108**, 063919 (2010).
- <sup>9</sup>E. Carpena, E. Mancini, D. Dazzi, C. Dallera, E. Puppini, and S. De Silvestri, *Phys. Rev. B* **81**, 060415 (2010).
- <sup>10</sup>D. Weller, O. Mosendz, G. Parker, S. Pisana, and T. S. Santos, *Phys. Status Solidi A* **210**, 1245 (2013).
- <sup>11</sup>O. Mosendz, S. Pisana, J. W. Reiner, B. Stipe, and D. Weller, *J. Appl. Phys.* **111**, 07B729 (2012).
- <sup>12</sup>B. M. Lairson, M. R. Visokay, R. Sinclair, and B. M. Clemens, *Appl. Phys. Lett.* **62**, 639 (1993).
- <sup>13</sup>A. Cebollada, D. Weller, J. Sticht, G. R. Harp, R. F. C. Farrow, R. F. Marks, R. Savoy, and J. C. Scott, *Phys. Rev. B* **50**, 3419 (1994).
- <sup>14</sup>O. A. Ivanov, L. Solina, V. Denshina, and L. Magat, *Phys. Met. Metallogr.* (English translation of *Fizika Metallov i Metallovedenie*) **35**, 81 (1973).
- <sup>15</sup>S. Okamoto, N. Kikuchi, O. Kitakami, T. Miyazaki, Y. Shimada, and K. Fukamichi, *Phys. Rev. B* **66**, 024413 (2002).
- <sup>16</sup>B. Marchon, T. Pitchford, Y.-T. Hsia, and S. Gangopadhyay, *Adv. Tribol.* **2013**, 1.
- <sup>17</sup>E. C. Stoner and E. P. Wohlfarth, *Philos. Trans. R. Soc., A* **240**, 599 (1948).
- <sup>18</sup>S. Wicht, V. Neu, L. Schultz, D. Weller, O. Mosendz, G. Parker, S. Pisana, and B. Rellinghaus, *J. Appl. Phys.* **114**, 063906 (2013).
- <sup>19</sup>P. Wolf, *J. Appl. Phys.* **32**, S95 (1961).
- <sup>20</sup>A. Barman, S. Wang, J. Maas, A. R. Hawkins, S. Kwon, J. Bokor, A. Liddle, and H. Schmidt, *Appl. Phys. Lett.* **90**, 202504 (2007).
- <sup>21</sup>M. Weisheit, M. Bonfim, R. Grechishkin, V. Barthem, S. Fahler, and D. Givord, *IEEE Trans. Magn.* **42**, 3072 (2006).
- <sup>22</sup>S. Mizukami, S. Iihama, N. Inami, T. Hiratsuka, G. Kim, H. Naganuma, M. Oogane, and Y. Ando, *Appl. Phys. Lett.* **98**, 052501 (2011).
- <sup>23</sup>P. He, X. Ma, J. W. Zhang, H. B. Zhao, G. Lüpke, Z. Shi, and S. M. Zhou, *Phys. Rev. Lett.* **110**, 077203 (2013).